Leibniz-Institut für Astrophysik Potsdam (AIP)
An der Sternwarte 16, D-14482 Potsdam, Germany
Tel: +49 (0) 331 7499 0, Fax: +49 (0) 331 7499 267

Natural Guide Star Tip-Tilt laboratory system characterization

Jesper Storm, & Dennis Plüschke

May 15, 2014
Large Binocular Telescope Project
ARGOS-TT-TEST-004 DRAFT v0.6
LBT-CAN-658g035a

Contents

1 Scope

We present the results from the laboratory characterization of the integrated ARGOS natural guide star tip-tilt system. This includes the different APD systems, fiber bundles and opto-mechanics.

2 Executive Summary

1. Bundle #2 has a peak QE of about 55% and an average QE of about 47% when disregarding APDs with poor performance
2. Bundle #2 exhibits no cross talk between channels
3. Bundle #2 provides the designed field of view
4. Bundle #2 shows an insignificant efficiency dip in the center of the array

3 The test setup

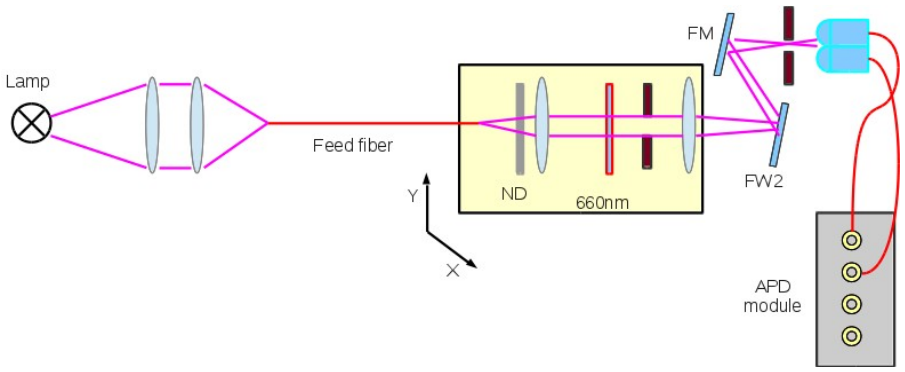

Figure 1: The test setup. The halogen lamp provides the light to the feed fiber. The end of the feed fiber is reimaged through a factor four beam expander, delivering an f/45 beam on the lenslets. The location of the ND filters and interference filters are shown. The mirrors in the filter wheel (FW2) and fold mirror (FM) are red pass mirrors surpressing the light blueward of 600nm. The fiber bundle from the lenslets to the APD module is also indicated.

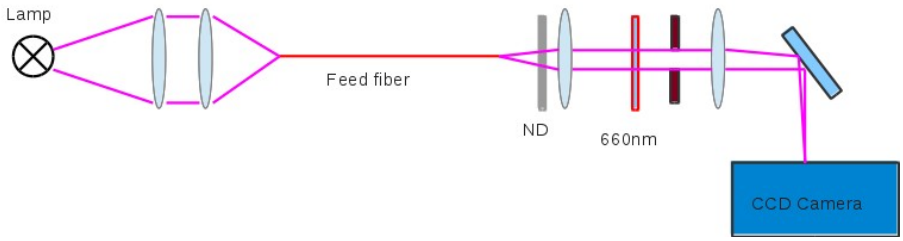

Figure 2: The reference test setup. Here the ARGOS TT system has been replaced by a CCD camera to provide a efficiency reference measurement.

The system was set up in the Faraday cage at the AIP as shown in Fig.1. A halogen lamp provided the light source which was fed through a feed fiber of either 105micron or 400micron diameter fiber. The fiber end was reimaged with a factor four beam expander to provide an f/45 beam (1800μm per arcsec) with a diameter of about 420 micron or 0.23 arcsec in the focal plane for the 105micron fiber, and a diameter of about 0.9arcsec for the 400micron fiber. The exit fiber end and beam expander were mounted on an X-Y stage (shown in pale yellow in Fig.1) to allow the image to be shifted in the focal plane. Note that the spot is tophat function being very flat across the aperture and then being cut off by the aperture edge. On sky the stars will be closer to a gaussian shape making the edges less sharp.
Using the Keyence camera and measurement system the aperture wheel and the lenslet array were adjusted to ensure that the lenslet array was centered in the largest aperture.
The filter wheel with the first fold mirror (FW2) was adjusted to place the spot in the center of the last fold mirror (FM) and the last fold mirror was adjusted to get the spot on the center of the lenslet array. The alignment will be described in a separate document.
The lenslet array with the associated fiber bundle was then connected to the APD unit. The APD unit was connected to the `argos-tt` laptop via ethernet over a switch and the USB output was connected to a USB tty port on the laptop as well.
The control electronics for the aperture wheel was connected via ethernet to the switch as well to enable control from the laptop.

4 Absolute efficiency of the long fiber bundles

Using a simple test setup with a laser diode we illuminated the fiber ends with an f/NN beam and measured the output with a power meter. The value was compared to the measured flux from the light source without the fiber in the beam. The fibers are uniform to within one percent and show an overall transmission of almost 95% at a wavelength of NNNnm. The values are tabulated in Tab.4. It was noticed that one fiber in teh first bundle was broken. This has been repaired but the throughput has not yet been verified.

5 Relative efficiencies of the APD modules

5.1 APD module #3

Again we used APD module #3 and we established the relative sensitivities of the channels by centering the light source on the lenslet array and setting the light level to about 10000cts/sec per

channel. We then measured the flux in all four channels (ch0,ch1,ch2,ch3) and then proceeded to shift all four fibers one position on the APD module. Repeating this process four times we had the flux from all four fibers on all four channels and we can compute the total flux in each channel after having subtracted the dark currect.
The dark current was measured to be 403, 423, 352, and 359 cts/sec in the four channels. The fluxes were measured to be:

```
13290.1 10567.8 10529.8 14019.9
12975.4 10734.5 11644.5 11300.8
12527.3 9956.53 12653.2 12441.5
13954.8 8983 10982.6 13834.4
```

leading to totals of:

```
51135.6 38549.8 44402.1 50160.6
```

and the relative efficiencies:

```
1.00 0.75 0.87 0.98
```

This module (#3) being our prototype module exhibits quite a variation, channel 1 being down by 25% compared to channel 0. These numbers are also summarized in the Appendix.

5.2 APD module #1

Later we did the same procedure for the APD module #1.
The dark current was measured to be 271, 355, 316, and 400cts/sec a bit higher than the specified 250cts/sec. This is most likely due to light in the lab. A separete measure of the dark current will be performed, but the values listed here are relevant for the relative efficiency measurements. Shifting the four fibers around the channels gave the following counts in 1sec:

```
Mean: 19 12753.7 11840.5 11754.2 15477.6
Mean: 19 10900.5 11629.4 15515.4 12954.7
Mean: 19 11094.3 16166.7 13498.3 11429.6
Mean: 19 13909.9 13455.5 11509.5 10499.7
```

As before the relative efficiencies could be determined to be 0.92, 1.00, 0.99, 0.94 so this array has a significantly more uniform response than unit #3 with a maximum difference of 8% between channels.

6 Bundle #2

Bundle #2 is the first science grade bundle and with the measuring setup having been established from the prototype system we could immediately proceed with characterizing the system.
First we investigate the efficiency of the system. This involves both the relative efficiency between the channels as well as the overall absolute efficiency of the system. In both cases the efficiency is affected on one hand by the performance of the APD's and on the other by the fiber bundles. Here we first investigate the relative efficiency of the APD's (Sec.5.1) and then we proceed with the relative efficiency of the fiber bundle #2 in Sec.6.1.

6.1 Relative efficiency of the bundle #2

.
To measure the relative efficiency of bundle #2 (`E13-040`) we proceeded as for the prototype bundle. We aligned the lenslet array with the fully open aperture in the aperture wheel. We used the large feed fiber with a diameter of 400μm , corresponding to a spot size of 0.9 arcsec on sky. We set the lamp voltage to the lowest setting of 3.2V and had the ND4 plus a 660/10nm narrow band filter in the beam. We used the long bundle `B13-329-01`, the APD module #3, the TT bundle #2 (`E13-040`) and the fibers were connected 1-1, 2-2, 3-3, 4-4, and the APD channels were connected F2-ch0, F3-ch1, F1-ch2, F4-ch3.
We measured the dark current as an average of 29 1sec integrations and found for ch0-3: 403,423,351, 359cts/sec respectively.

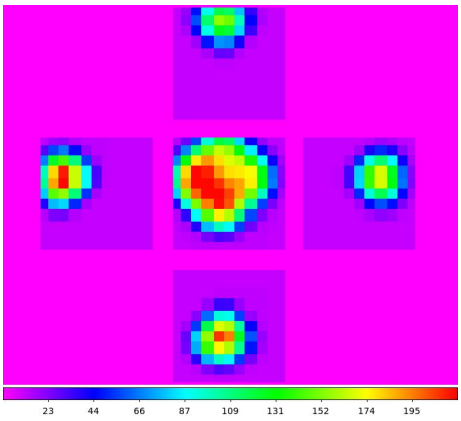

Figure 3: The signal as a function of (x,y) position in a raster scan with step size 500μm . The outer four images represent the response of the individual channels while the center image is the sum of the four outer images and thus representing the overall sensitivity of the array. In this case the channels have been dark subtracted and corrected for the APD flatfield leaving the relative sensitivities. The intensity scale ranges from -0.05 to 1.0.

We then made a raster scan with step size 500μm (raster20140417a.log) and 11 by 11 pixels centered roughly on (X,Y)=(6.8,6.3). For each channel we could then make an image showing the intensity for a given raster position after subtracting the dark current and dividing out the relative efficiency of the APD's from the previous section. The images are shown in Fig.3 as the outer four images and in the center the sum of the four outer images is displayed as well showing the overall efficiency as a function of raster position. The relative efficiency of the bundle has been estimated from the peak intensity in each of the channels as we find it to be 1.0, 0.71, 0.96, 0.77 for fibers 1 through 4. This suggests that the bundle looses almost 30% of the light in the lenslets 2 and 4 whereas 1 and three are in good agreement. The effect is easily correcetd for by dividing by these relative efficiencies as can be seen in Fig.4.
The test was repeated with the APD module #1 but using the smaller step size in the scan, so not covering the complete field of view. The general result could be verified and we found in this case relative efficiencies based on the peak counts in the channels of 0.85, 0.68, 0.95, 1.00. ch1 is again low by about 30% w.r.t. best channel, but ch4 is now the best channel and not down by 25% as suggested above. However, as we did not cover the full FOV we did not cover

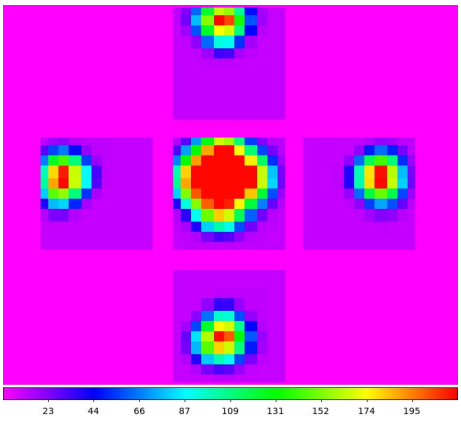

Figure 4: As in the previous figure. In this case the channels have been flatfielded. The intensity scale ranges from −0.05 to 1.0.

the peak response of all the lenslets, so this result does not carry much weight and only serves to verify the previous findings.
We note that the raster scan reveals the shape of the lenslet array as a square which is rotated by 45 degrees w.r.t. scan axes. This can be seen both for the individual lenses as well as for the lenslet array itself. We also not that in the final 'flat fielded' summed image the central part is very smooth, showing the we do not have a significant sensitivity deficit in the center. This is better explored with the smaller feed fiber (see below).
Note that the 90% level extends over 7 pixels in the diagonal, or 5 pixels on the side. This is about 2.5mm or 1.4arcsec in the sky. Considering that the beam is roughly 1arcsec wide this corresponds to the expected field of view of more than 2 by 2 arcsec as we only start to loose light when the beam starts to fall off the edge of the lenslet array. Looking at the 50% levels which extends at 10pixels in the diagonal of 7 pixels on the side or 2 by 2arcsec on the side we can confirm this effective field of view.
To further investigate the behaviour around the central position a finer raster with 250μm steps was obtained. The result is shown in Fig.5. The central image is the sum of the four channels, the intensity scale ranges from 0.7 to 1.1 for the central image and it is obvious that there is NO significant dip in sensitivity in the center of the array for a 0.9 arcsec spot.
Using the 105μm feed fiber, corresponding to a 0.23arcsec spot, we redid the finer raster (`raster20140409c.log`) and came up with the images in Fig.6. It can be seen that in the center there is a fall off in efficiency of the order 25%. A trace through the central line in the summed image is shown in Fig.7. Note that the step size if 250μm or 0.13arcsec in the sky.

6.2 Absolute efficiency of Bundle #2

To determine the overall absolute efficiency we have used a CCD camera with a known QE to determine the available photon flux in the above laboratory setup. We replaced the ARGOS components shown in Fig.1 with a fold mirror and our Apogee CCD camera as shown in Fig.2. We made transfer curve measurements for the camera to determine the conversion factor from ADU to electrons and found a value of $0.96 \pm 0.01 e^-$ /ADU. The Apogee QE curve shows a value of 90% at 660nm. In the setup above the Apogee camera collected 994000ADU in 10sec (image:

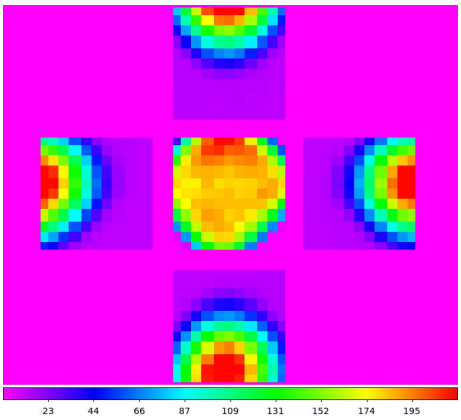

Figure 5: The signal as a function of (x,y) position in a raster scan with step size 250μm using the 0.9 arcsec spot. The outer four images represent the response of the individual channels while the center image is the sum of the four outer images and thus representing the overall sensitivity of the array. In this case the channels have been dark subtracted and flat fielded. The intensity scale ranges from -0.05 to 1.0 for the outer images whereas the summed image in the center ranges from 0.7 to 1.1 to better show the very limited variation across the field of view.

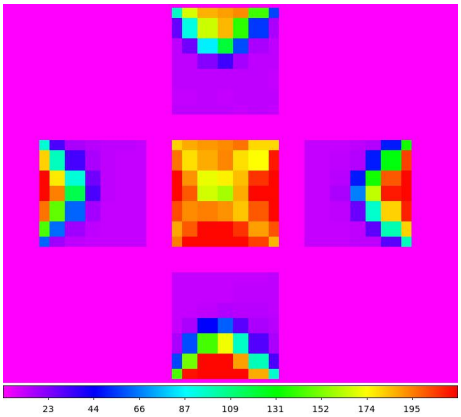

Figure 6: The signal as a function of (x,y) position in a 7x7 raster scan with step size 250μm and in this case using the small feed fiber corresponding to a 0.23arcsec spot. The outer four images represent the response of the individual channels while the center image is the sum of the four outer images and thus representing the overall sensitivity of the array. In this case the channels have been dark subtracted and flat fielded. The intensity scale ranges from -0.05 to 1.0 for all the images.

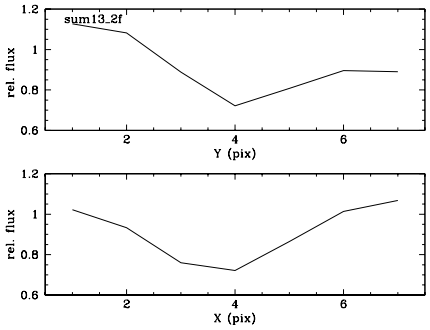

Figure 7: The relative flux as a function of x and y position in the central row and column of the previous summed image. The raster step size is 250μm (0.13arcsec) and the feedfiber is 105μm or 0.23arcsec in the sky.

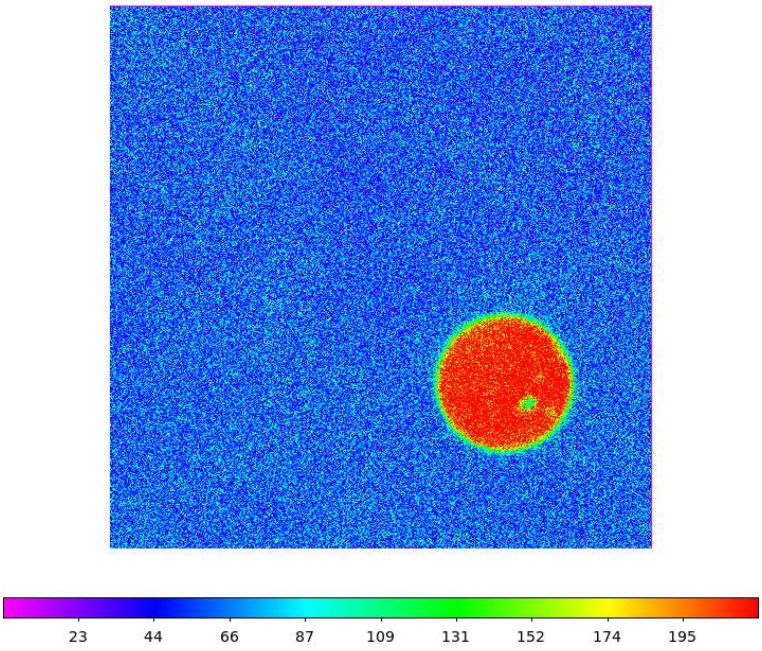

Figure 8: The pinhole image on the Apogee camera. The smooth illumination is obvious as is the sharp edges of the spot.

`light_ND4_660nm_32V_10s_400m_1x1.fits`) or $95440e^-$ /sec after correcting for the background counts and applying the conversion factor. We correct for the 90% QE, 98% entrace window, 96% fold mirror and find a flux of $95440/(0.90 \times 0.98 \times 0.96) = 112720$ph/sec. The CCD appears to be very flat in the response so no flat field correction has been applied.
We can compare this number with the value from the bundle#2 when we have subtracted the dark and corrected for the relative efficiencies of the APD's, that is we have normalized to the most sensitive APD. This is the image `sum15_bf` which has the peak value of 61953cts/sec. This corresponds to a peak efficiency of $61953/112720 \times 100 = 55\%$. Considering that the APD's have a QE of about 60% at 660nm we are close to this value and have losses in the optics of the order 10%. These losses can be ascribed to the various interfaces in the beam. We have the two fold mirrors, the lenslet, the lenslet-fiber coupling (glued), the fiber to fiber coupling and the fiber to APD coupling. Within the errors it looks very reasonable, suggesting that we are not wasting photons. At the same time it is clear that some of the channels have a lowered efficiency by up to 30% with respect to the peak. For all channels together this sums up to a loss of about 15% which folded with the 55% peak QE of the system including the APDs gives a total system QE of $(1.00 - 0.15) \times 0.55 = 47\%$. These additional losses are most likely due to slight mismatches between the fibers and the exit pupils of the lenslets. The good performance requires APD's which performs well. In module #3 a couple of the APDs have reduced performance (by about 25%) which of course will further impact the performance on sky. This is also the prototype module with the higher dark current.
The design goal of this part of the system (ARGOS-FDR-18) was a throughput from the pickup mirror in the technical arm to the APD sensor of 83% and a conservative estimate of 70% and including the APD QE of 60% these values transform into 50% and 42%. The measured value of 47% is thus in between our conservative and optimistic design goal with a good APD module (but not with #3!). Note that we have not applied optics gel to the fiber coupling between the bundle and the long fibers. This ought to improve the sensitivity by another few percent. (Still TBD).

7 Guiding sensitivity

The TT module computes on the basis of the counts in the four channels the guiding signal $(\Delta X, \Delta Y)$ and rotates it according to the rotation of the lenslet array with respect to the x,y directions. In the present case the angle is close to 45 degrees. In Fig.9 the guiding signal has been plotted as a function of the XY coordinate in the scan in the images in the upper row. The left images show the offset in X and the right hand images show the offset in Y. These signals are based on the images from the previous section obtained with the 400μm feed fiber corresponding to a 0.9arcsec spot on the lenslet array.
The lower row of images show the guide signal as computed on basis of the raster scans from above using IRAF using the formula:

$$\Delta x = [(C_2 + C_4) - (C_1 + C_3)]/\sum_n C_n \quad (1)$$

$$\Delta y = [(C_1 + C_2) - (C_3 + C_4)]/\sum_n C_n \quad (2)$$

$$(3)$$

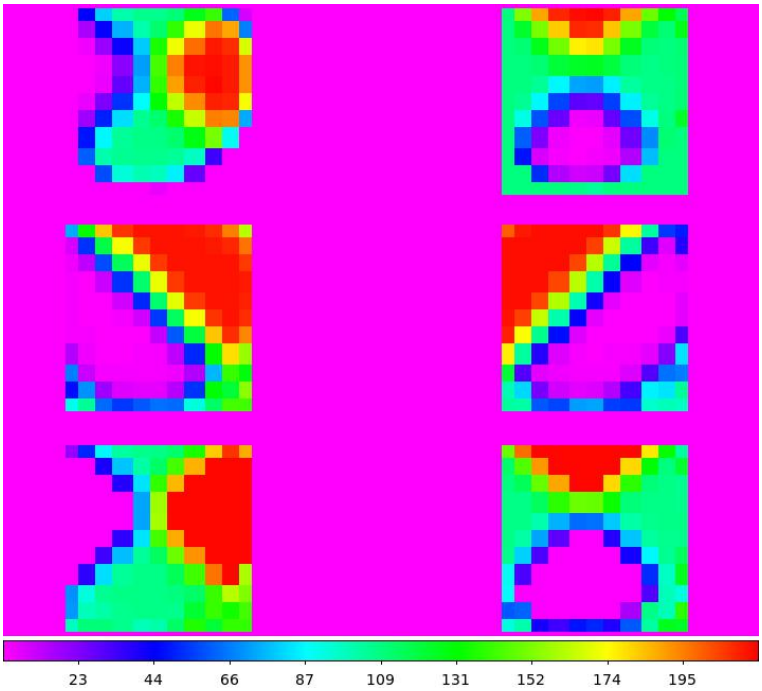

Figure 9: The guide signal as a function of raster position. The middle row of images show the offsets in X (left) and in Y (right) as a function of raster position. The upper row shows the offsets in X (left) and Y (right) after the rotation of 45 degrees has been taken out by the TT computer. The lower row is the same as the upper row except that the computations have been done directly from the images in the middle row.

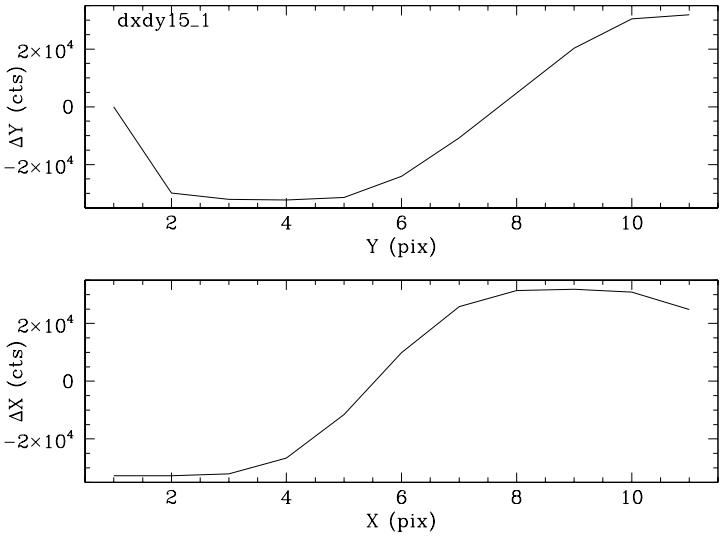

Figure 10: The guide signal in counts as a function of the X and Y position, based on row 8 in the upper left image (dx15_1; X-offset) of the previous figure and based on column 5 in the upper right (dy15_1; Y-offset) of the previous figure.

where C_n are the counts in the different channels corrected for dark current, background and flatfield. The offsets are then rotated using the known rotation angle α.
It can be seen that these images are in good agreement with the upper row of images computed by the TT computer on the fly. The central row of images have been computed without applying the rotation and the 45 degree rotation angle is evident.
We note that the structure of the rotated signals is more complex than the simple case as seen in the middle row. This is due to the fact that the quad cell does not allow for the determination of a centroid position and can only be efficient when the target is well centered.
For the well centered case we have determined the response of ΔX vs X and ΔY versus Y from the images in the upper row of Fig.9 by plotting (in Fig.10) the row 8 of the dx image and column 5 in the dy image. Fitting a straight line to the almost linear part gives slopes of 18000cts/pix in X and 17000 cts/pix in Y. We note that the slope changes when moving off the center. This can easily explain the slight difference between the two directions and the relevant number is the maximum value which can be achieved. 18000cts/pix with pixels of 500μm results in 18000cts per 0.28arcsec or 64000cts/arcsec. A higher background relative to the brightness of the star will lead to a lower value. A larger seeing disk will also lead to a lower value.

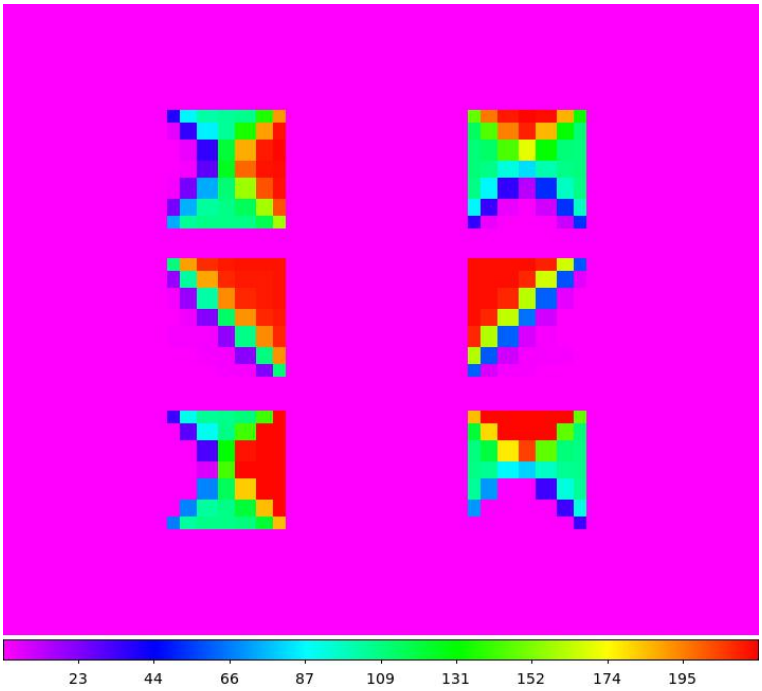

Figure 11: The guide signal as a function of raster position for the small feed fiber with the 0.23arcsec spot size. The raster had steps of 250μm .

The experiment was repeated using the small feed fiber with the 0.23arcsec spot size and raster step size of 250μm . The results are shown in Fig.11 and Fig.12. In this case the slopes were about 25000cts/pix. With one pixel being 250μm or 0.14arcsec this results in a slope of 180000cts/arcsec. This is a factor 2.8 more than with the 0.9arcsec spot, a bit less than the zero'th order estimate of a factor of 3.8.

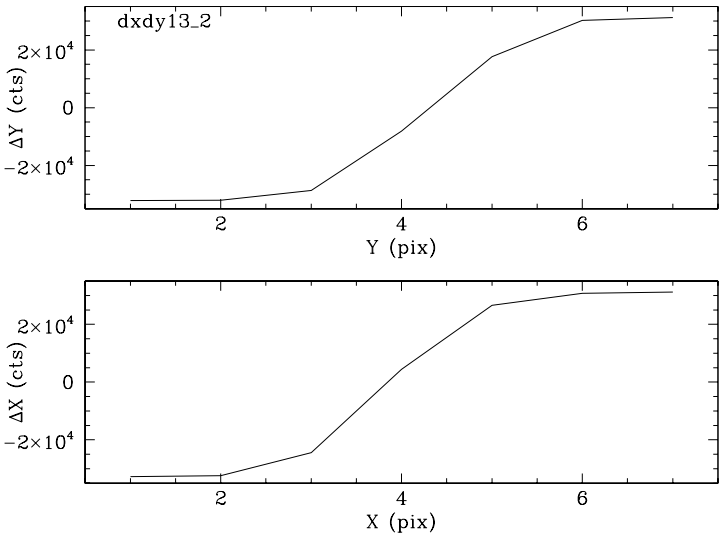

Figure 12: The guide signal in counts as a function of the X and Y position, based on row 4 in the upper left image (dx13_2; X-offset) of the previous figure and based on column 4 in the upper right (dy13_2; Y-offset) of the previous figure.

8 Time sequences

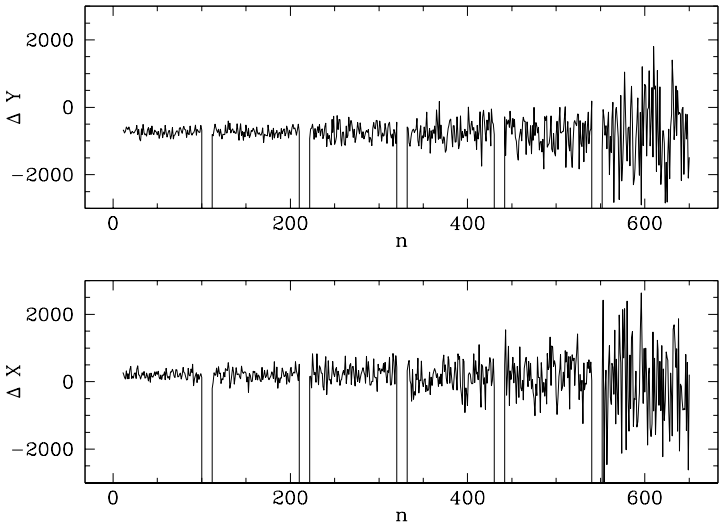

Figure 13: The guide signal in counts in X and Y as a function of sample number (n) for different integrration times. From left to right the integration times are 1000, 500, 200, 100, 50, and 10ms.

Table 1: The RMS values on the measured guide corrections for different integration times. The total detected flux was 48000cts/sec.

Integration time	Number of samples	ΔX	RMS(ΔX)	ΔY	RMS(ΔY)
10	2999	147.535	1190.52	-745.979	1069.7
50	1299	192.075	523.757	-754.736	482.712
100	599	184.746	390.412	-734.791	326.05
200	299	224.702	264.436	-745.505	223.49
500	169	198.367	166.25	-737.929	139.795
1000	99	205.545	114.869	-725.717	105.119
msec		cts	cts	cts	cts

To determined the noise in the guiding signal a number of time sequences were recorded with different integration times with the large feed fiber (0.9arcsec spot size). The first hundred samples of each time sequence is plotted consecutively in Fig.13. As expected the RMS scatter increases as the integration time is lowered. The detected flux in this experiment was a total of 48000cts/sec distributed over the four channels.

For each integration time the RMS scatter was computed and tabulated together with the guiding offset in Tab.1. Considering the gain found in Sec.7 of 64000cts/arcsec an RMS value of 1000 corresponds to a jitter of 0.015 arcsec. The RMS values in X and Y are plotted in Fig.14. The differences in the guiding offsets between the different integration times is less than 50cts (0.0008arcsec with the 64000cts/arcsec conversion factor) which is totally negligible.

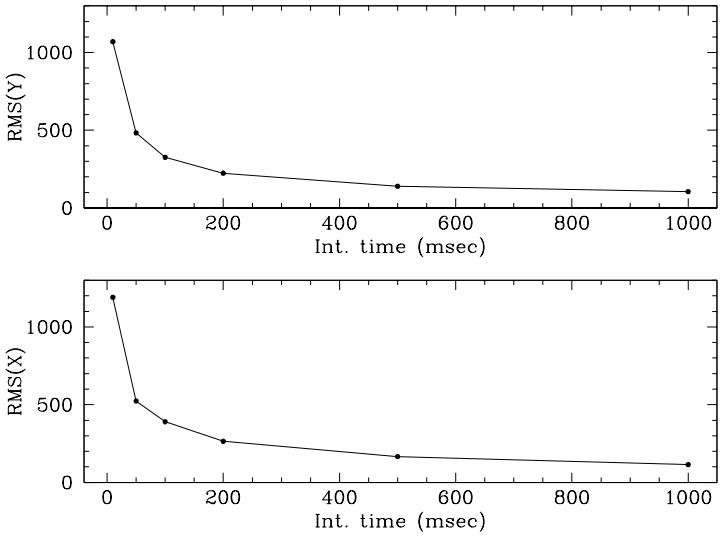

Figure 14: The RMS value on the guide signal for different integration times.

A detected flux of 48000cts/sec with an estimated efficiency of 50% corresponds to about 100kcts/sec. This is about 10 times more than the existing off-axis guider camera detects for an 18mag star. Assuming we have the same overall detective quantum efficiency as the off-axis guider (admittedly a rather crude assumption) this would correspond to a star with a magnitude of $r' = 15.5$ mag.

A Relative efficiencies

Table 2: Relative efficiencies for the channels of the APD modules as measured in the lab.

Module	ch0	ch1	ch2	ch3
#1	0.92	1.00	0.99	0.95
#2				
#3	1.00	0.75	0.87	0.98
#4				

Table 3: Relative efficiencies for the lenslet bundles as measured in the lab.

	Lenslet			
Bundle	1	2	3	4
#0 (prototype)	1.00	0.87	0.34	0.70
#1 (`E13-NNN` + `B12-160/02`)				
#2 (`E13-040` + `B13-329/01`)	1.00	0.71	0.96	0.77

Table 4: Absolute efficiencies for the long fiber bundles.

	Fiber			
Bundle	1	2	3	4
B12-160/01	–	–	broken	–
B12-160/02	94.6	94.8	94.9	94.9
B13-329/01	94.9	94.9	94.5	95.0
B13-329/02	95.1	94.8	95.1	94.4
	%	%	%	%